Core excitations and narrow states beyond the proton dripline: The exotic nucleus ^{21}Al

N. K. Timofeyuk,[1] B. Fernández-Domínguez,[2] P. Descouvemont,[3] W. N. Catford,[1] F. Delaunay,[4] and J. S. Thomas[1,*]

[1]*Department of Physics, Faculty of Electronics and Physical Sciences, University of Surrey, Guildford, GU2 7XH, United Kingdom*

[2]*Universidade de Santiago de Compostela, E-15754 Santiago de Compostela, Spain*

[3]*PNTPM, C.P. 229, Université Libre de Bruxelles, B-1050 Brussels, Belgium*

[4]*LPC Caen, ENSICAEN, Université de Caen, CNRS/IN2P3, F-14050 Caen, France*

(Received 22 May 2012; revised manuscript received 9 July 2012; published 5 September 2012)

We present the first predictions for the widths of resonance states in a so-far unobserved exotic isotope beyond the proton dripline, ^{21}Al. For this purpose we employ mirror symmetry between the widths of low-lying resonance states and the asymptotic normalization coefficients (ANC) of their mirror analogs. The latter are extracted from a recently measured peripheral reaction ^{20}O$(d,p)^{21}$O while the positions of resonances are estimated within a microscopic cluster model and a two-body potential model. We have found that ^{21}Al should have two low-lying states decaying into the ^{20}Mg $+ p$ channel and three states at higher energy, built on the 2^+ core excited state and decaying into the ^{20}Mg$(2^+) + p$ channel. The widths of all these states are much smaller than their energies, which makes experimental spectroscopic studies of this isotope beyond the proton dripline possible.

DOI: 10.1103/PhysRevC.86.034305 PACS number(s): 21.10.Jx, 21.60.Gx, 23.50.+z, 27.30.+t

I. INTRODUCTION

Modern experimental techniques study the limits of nuclear existence on both the neutron- and the proton-rich side. In the light nuclear mass region, the proton dripline was mainly identified and the cutting-edge experimental studies probe the structure beyond this line. Although in this region the nuclei quite often exist as broad resonances (like ^{10,11}N, ^{14,15}F) due to the Coulomb barrier being insufficient to hold the proton for a long time, some nuclear resonant states may be very narrow [1]. This can arise from a peculiar structure of such states wherein a few nucleons move around an excited core so that the main decay channel has much smaller energy and thus is held longer by the Coulomb barrier [2]. Experimentally, the existence of several such states was confirmed in ^{15}F, ^{16}Ne [2], and in ^{19}Na [3]. Theory also predicts narrow states in ^{17}Na (the mirror analog of ^{17}C) due to a large amplitude of the core excitations [4]. In this paper, we highlight a yet nonobserved isotope beyond the proton dripline, ^{21}Al, which may include unexpectedly long-lived states in its spectrum due to core excitation effects.

In the simplest model, ^{21}Al has eight neutrons and eight protons fully occupying the $0s$ and $0p$ closed shells, and five protons in the $d_{5/2}$ shell, so that it is expected to have spin and parity $5/2^+$, the same as its mirror analog ^{21}O. The only known experimental information about ^{21}Al is that it lives less than 35 ns [5], which corresponds to the proton decay width larger than 1.3×10^{-8} eV. According to mass systematics, the ^{21}Al ground state is unbound with respect to proton emission by 1.26(30) MeV [6]. Detailed analyses of Coulomb displacement energies give similar separation energies in ^{21}Al, 1.286(30), 1.254(50), and 1.468(40) MeV [7]. Two theoretical calculations for ^{21}Al binding energy have been published. The supersymmetrical IBM4 model claims that the difference in binding energies of ^{21}Al and ^{19}Na is 140 keV [8], which (combined with the known proton binding in ^{20}Mg) means that ^{21}Al is unbound by 2.5 MeV. However, spherical Hartree-Fock-Bogolyubov calculations suggest that it might be bound by 480 keV [7].

In the present paper, we estimate energies of the ^{21}Al resonances within a two-cluster microscopic cluster model (MCM). Using experimental values of asymptotic normalization coefficients (ANCs) for mirror states in ^{21}O we then predict the widths of the ^{21}Al states. We also present estimates within a simple potential model.

II. SYMMETRY RELATIONS IN UNBOUND-BOUND MIRROR PAIRS

In bound-unbound mirror pairs, the width Γ_p of a proton resonance is linked to the ANC C_n of its mirror bound analog by an approximate equation [9]:

$$\frac{\Gamma_p}{C_n^2} \approx \frac{\hbar^2 \kappa_p}{\mu} \left| \frac{F_l(\kappa_p R_N)}{\kappa_p R_N \; j_l(i\kappa_n R_N)} \right|^2, \qquad (1)$$

where $\kappa_{p(n)} = \sqrt{2\mu\epsilon_{p(n)}}/\hbar$, $\epsilon_{p(n)}$ is the energy of the proton resonance (neutron separation energy), μ is the reduced mass for the last nucleon plus core, l is the orbital momentum, F_l is the regular Coulomb wave function, j_l is the spherical Bessel function, and R_N is the range of the nuclear interaction between the last nucleon and the core. The choice $R_N = 1.3 \times (A-1)^{1/3}$ fm minimizes the error of the approximation in Eq. (1) [10]. C_n is defined via asymptotics of the radial overlap integral $I_{lj}(r)$ between nuclei A and $A-1$:

$$I_{lj}(r) \to i^{l+1} C_n \kappa_n h_l^{(1)}(i\kappa_n r), \quad r \to \infty, \qquad (2)$$

where r is the distance between the last neutron and $A-1$ and $h_l^{(1)}$ is the Hankel function of the first kind.

*Present address: Schuster Laboratory, University of Manchester, Manchester, M13 9PL, UK.

III. DETERMINATION OF ^{21}O ANCS FROM THE $^{21}O(d,p)^{20}$O REACTION

The ANCs C_n can be determined from the transfer reaction $^{20}\mathrm{O}(d,p)^{21}\mathrm{O}$, the amplitude of which contains the overlap $I_{lj}(r)$. The angular distributions of this reaction have been measured and analyzed in Ref. [11] in terms of spectroscopic factors with an emphasis on the onset of the $N = 16$ gap emergence in ^{21}O, but no ANCs were reported. In the present paper we reanalyze the data in terms of ANCs using the same reaction theory as in Ref. [11]. We perform the transfer calculations with several values of the radius r_0 of the transferred neutron potential well to show that unlike the spectroscopic factor, the ANC does not depend on this choice (see Fig. 1). Such a feature is typical for peripheral reactions that are dominated by $r > R_N$. The ANCs are, therefore, reliably extracted and the values for two states below the threshold of neutron emission, the $5/2^+$ ground state and the $1/2^+$ first excited state, are given in Table I.

The $^{20}\mathrm{O}(d,p)^{21}\mathrm{O}$ experiment showed no evidence for the three other bound levels known in the ^{21}O spectrum at 2.13, 3.026, and 3.073 MeV [5]. The first one most likely corresponds to the $3/2^+_1$ state predicted by the shell model WBP calculation [12], while the two other nearly degenerate levels are most likely $5/2^+_2$ and $7/2^+_1$ (see Fig. 3). According to the shell model, these states are built on core excited states (see Table II). Their mirrors are thus strong candidates for narrow states in the proton continuum, living longer due to suppression of the decay into the ground-state channel. From nonobservation of these levels in ^{21}O, we have obtained in Table I the upper limits for the corresponding ANCs. The ANC values for $^{21}\mathrm{O} \to {}^{20}\mathrm{O}(2^+) + n$ presented there are needed to estimate the width of the $^{21}\mathrm{Al} \to {}^{20}\mathrm{Mg}(2^+) + p$ decay. They were obtained from an analysis of sequential transfer via excited $^{20}\mathrm{O}(2^+)$ state, $^{20}\mathrm{O}(d,d')^{20}\mathrm{O}(2^+)(d,p)^{21}\mathrm{O}^*$ using the coupled-channel Born approximation in which only three partitions are left: $^{20}O + d$, $^{20}\mathrm{O}(2^+) + d$, and $^{21}\mathrm{O}(J^\pi_f) + p$.

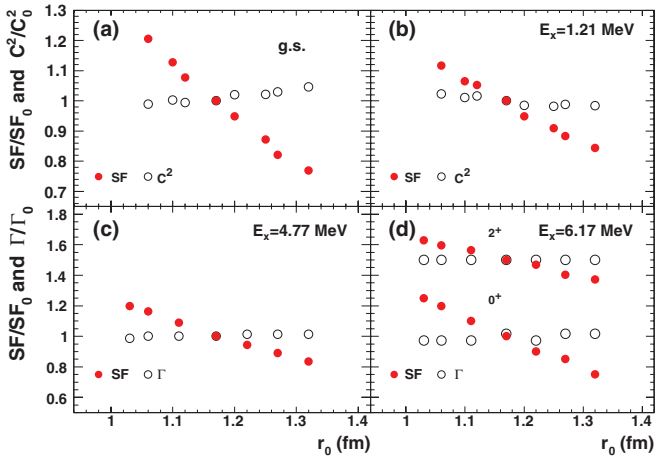

FIG. 1. (Color online) Spectroscopic factors (a)–(d), ANCs for bound (a) and (b), and neutron widths for unbound (c) and (d) states of ^{21}O obtained for various radii r_0 of the neutron potential well and shown as ratios to the values S_0, C_0^2, and Γ_0 obtained with $r_0 = 1.17$ fm used in previous study in Ref. [11].

TABLE I. Squared ANCs C_n^2 (in fm^{-1}) obtained from the $^{20}\mathrm{O}(J^\pi_i)(d,p)^{21}\mathrm{O}(J^\pi_f)$ reaction and from the MCM.

J^π_f	J^π_i	lj	(d,p)	Multichannel MCM	Single-channel MCM
$5/2^+_1$	0^+	$d_{5/2}$	0.22 ± 0.05	0.25	0.30
$1/2^+_1$	0^+	$s_{1/2}$	5.06 ± 1.24	6.4	6.9
$3/2^+_1$	0^+	$d_{3/2}$	$\leqslant 7.0 \times 10^{-5}$	6×10^{-3}	
$5/2^+_2$	0^+	$d_{5/2}$	$\leqslant 4.2 \times 10^{-4}$	3.6×10^{-4}	
$7/2^+_1$	0^+	$g_{7/2}$	$\leqslant 5.6 \times 10^{-9}$	6.4×10^{-11}	
$3/2^+_1$	2^+	$s_{1/2}$	$\leqslant 3.20$	10.4	
$5/2^+_2$	2^+	$s_{1/2}$	$\leqslant 104$		5.42
$7/2^+_1$	2^+	$d_{3/2}$	$\leqslant 0.050$		6×10^{-4}
	2^+	$d_{5/2}$	$\leqslant 0.115$		0.2362

The overlap $\langle {}^{21}\mathrm{O}(J^\pi_f)|{}^{20}\mathrm{O}(0^+)\rangle$ was assumed to be zero for this purpose.

Using the ^{21}O ANCs, Eq. (1) gives the widths of the mirror proton resonances in ^{21}Al (or their upper limits) as functions of ϵ_p. These widths, denoted as $\Gamma^{(dp)}$ to stress that they have been obtained from ANCs extracted from (d,p) reactions, are plotted in Fig. 2. They increase dramatically as ϵ_p approaches the Coulomb barrier. For $\epsilon_p = 1.3$ MeV from mass systematics, the width $\Gamma^{(dp)}$ of $^{21}\mathrm{Al}(5/2^+_1)$ is equal to 1 keV.

IV. CALCULATIONS OF ^{21}Al ENERGIES IN THE MICROSCOPIC CLUSTER MODEL

To calculate the energies of the ^{21}Al states, it is crucial to use the model that can treat correct asymptotic behavior of the last proton as it is expected to be in the continuum. Today, the most advanced many-body methods with modern *NN* interactions cannot yet deal with the proper asymptotic behavior in the *sd* shell with several nucleons in it. Therefore, we use the microscopic cluster model, well adapted for these purposes.

The MCM generates a cluster approximation of the many-body wave function for the Hamiltonian,

$$H = \sum_{i=1}^{A} T_i + \sum_{j>i=1}^{A} V_{ij}, \tag{3}$$

where T_i is the kinetic energy of nucleon i, and V_{ij} is a nucleon-nucleon (*NN*) interaction. In this approximation the wave function in partial wave J^π with the relative angular momentum l and the channel spin I reads

$$\Psi^{JM\pi} = \sum_{I_C l I} \mathcal{A}\left[Y_l(\Omega_\rho) \otimes \left[\phi_C^{I_C} \otimes \phi_n\right]^I\right]^{JM} g^{J\pi}_{I_C l I}(\rho). \tag{4}$$

Here I_C is the spin of ^{20}O (or ^{20}Mg), $\phi_C^{I_C}$ and ϕ_n are the internal wave functions of the clusters ^{20}O (^{20}Mg) and neutron (proton), $g^{J\pi}_{I_C l I}(\rho)$ is the radial function depending on the relative coordinate ρ, and $\mathcal{A}$ is the antisymmetrization operator. The asymptotic behavior at large ρ, crucial for weakly bound and unbound nucleons, is taken exactly into account through the *R*-matrix method. The single-particle wave functions in ^{20}O

TABLE II. Spectroscopic factors $S = \sum_{lj} S_{l,j}$ for the $\langle {}^{20}\mathrm{O}(J_i)|{}^{21}\mathrm{O}(J_f)\rangle$ overlap calculated in the shell model with WBP interaction and within the MCM with V2 using sets A and B for the $5/2^+$, $1/2^+$ and $3/2^+$, $7/2^+$, $9/2^+$ states, respectively.

	Shell model						MCM					
J_f J_i	0^+_1	0^+_2	2^+_1	2^+_2	4^+_1	4^+_2	0^+_1	0^+_2	2^+_1	2^+_2	4^+_1	4^+_2
$5/2^+_1$	0.345	10^{-4}	1.30	0.148	2.60	0.022	0.314	$\times 10^{-5}$	1.306	0.061	2.192	0.001
$1/2^+_1$	0.811	0.137	0.286	1.03			0.881	0.048	0.170	0.967	0.002	3×10^{-4}
$3/2^+_1$	2×10^{-5}	0.008	0.751	1.42	0.022	1.09	0.004	0.005	0.836	0.801	0.03	0.886
$7/2^+_1$			0.199	0.430	0.847	1.962	8×10^{-5}	2×10^{-5}	0.059	0.468	0.822	1.660
$5/2^+_2$	0.036	0.502	0.896	0.053	0.033	0.192	0.024	0.084	0.879	0.012	0.047	0.120
$9/2^+_1$			5×10^{-4}	0.259	0.829	0.261	2×10^{-5}	8×10^{-5}	0.03	0.019	1.041	0.268
$3/2^+_2$	0.846	0.112	0.076	0.012	0.085	0.039	0.927	3×10^{-4}	0.113	0.013	0.052	0.071
$5/2^+_3$	0.004	0.386	0.053	0.610	0.107	0.018	0.002	0.036	0.742	0.100	0.174	0.053
$3/2^+_3$	0.028	0.007	0.509	0.053	0.029	0.077	0.116	4×10^{-4}	0.967	0.010	0.073	0.010
$7/2^+_2$			0.939	0.015	0.003	0.019	1×10^{-5}	7×10^{-6}	1.017	0.005	0.017	0.028

that make up $\phi_C^{I_C}$ are taken from the oscillator shell model with the oscillator radius of 1.7 fm. The four valence neutrons in the ^{20}O core were allowed occupy the $0d_{5/2}$, $1s_{1/2}$, and $0d_{3/2}$ orbitals, which gives many excitations in ^{20}O. We consider only the $0^+_{1,2,3}$, $2^+_{1,2,3,4}$, 3^+_1, and $4^+_{1,2,3}$ states that give the most important contributions.

The choice of the model dictates the choice of the *NN* interactions to be consistent with it. The effective Volkov forces [13] suit this model very well. In this work, we use Volkov V2 plus a zero-range spin-orbit force with an adjustable depth S_0 [14]. The V2 has another adjustable parameter, the Majorana exchange parameter m that determines the strength of the *NN* potentials in odd partial waves. Usually, S_0 is fixed to reproduce the excitation energy of the core of one of the clusters. However, the excitation energy of ^{20}O(2^+), calculated with V2, is not sensitive to S_0 for all m being smaller than the experimental one by 140–230 keV. Thus, other criteria to fix S_0 were used. It is possible to choose S_0 in such a way that the splitting between $5/2^+$ and $1/2^+$ in ^{21}O is reproduced. However, it gives low the energies of $3/2^+_1$ and $7/2^+$. Another

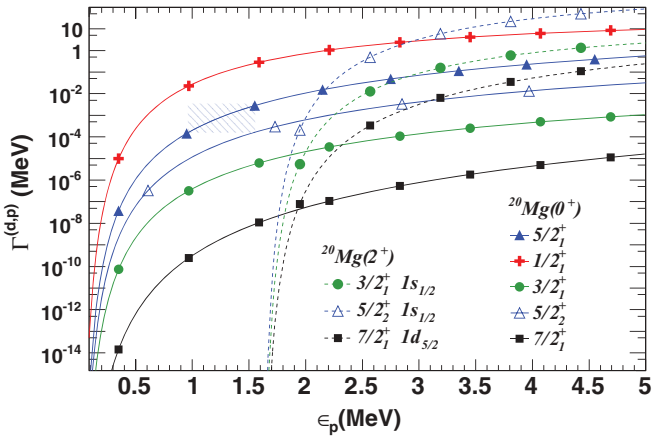

FIG. 2. (Color online) Resonance widths (or their upper limits) for decay of mirror analogs of the ^{21}O bound states into the ^{20}Mg(0^+) + p and ^{20}Mg(2^+) + p channels shown as functions of the resonance energy ϵ_p. The square box shows the widths corresponding to the ^{21}Al ground-state energy obtained from mass systematics.

choice is to reproduce the splitting between $3/2^+_1$ and $3/2^+_2$, however, this raises significantly the $1/2^+_1$ level. This is the consequence of the $5/2^+$, $1/2^+$ and the $3/2^+$, $7/2^+$, $9/2^+$ groups of states being built on the ^{20}O(0^+) and ^{20}O(2^+) states, respectively (see Table II for MCM predictions). Because the core excitation energy cannot be reproduced with the present model, it is impossible to get one set of m and S_0 that gives simultaneously a good spectrum both for the $5/2^+$, $1/2^+$ and the $3/2^+$, $7/2^+$, $9/2^+$ groups of states as well. As a result, we use below two sets of m and S_0: (A) $m = 0.65103$, $S_0 = 24$ MeV fm^5 and (B) $m = 0.6727$, $S_0 = 32.88$ MeV fm^5. Set A reproduces the separation energies of $5/2^+_{1,2}$ and $1/2^+_1$ and gives the excitation energy of $5/2^+_3$ close to the shell model predictions. Set B reproduces the energies of $3/2^+_{1,2}$ and predicts reasonable excitation energies of the $7/2^+_{1,2}$ and $9/2^+$ levels (see Fig. 3).

The ANCs calculated in the MCM for $5/2^+$, $1/2^+$ and $3/2^+$, $7/2^+$ with the sets A and B, respectively, are shown in Table I (to get a meaningful value of the ANC for the $7/2^+_1$ state we had to slightly modify the value m to reproduce its experimental energy).

The ANCs for $5/2^+_{1,2}$ and $7/2^+$ are within the experimental limits; the $1/2^+_1$ ANC is slightly larger than the experimental one. The ANC for the $3/2^+_1$ is very small in absolute terms, so the difference with experiment is not significant.

Using sets A and B we have predicted the ^{21}Al spectrum in the MCM (see Table III). The ^{21}Al ground state turns out to lie unexpectedly low, just 80 keV above the ^{20}Mg + p threshold, $\sim$1 MeV below the mass systematics prediction. As a consequence, it has a tiny width, 2.1×10^{-17} MeV that corresponds to a lifetime of 26 μs, which is much longer than the experimentally estimated upper limit of 35 ns [5]. However, slightly changing the Majorana parameter m to increase the ^{21}Al ground-state energy by only 35 keV brings the lifetime of ^{21}Al within the experimental limits.

To investigate why MCM predicts a very low energy ϵ_p for ^{21}Al(g.s.), the effect of the channels with core excited states was studied. If they all are neglected in the expansion (4) then ϵ_p increases to 1.13 MeV (see Table III) which is close to the prediction from mass systematics. Adding just two channels with ^{20}Mg(2^+) and ^{20}Mg(4^+) restores the low value of ϵ_p. The

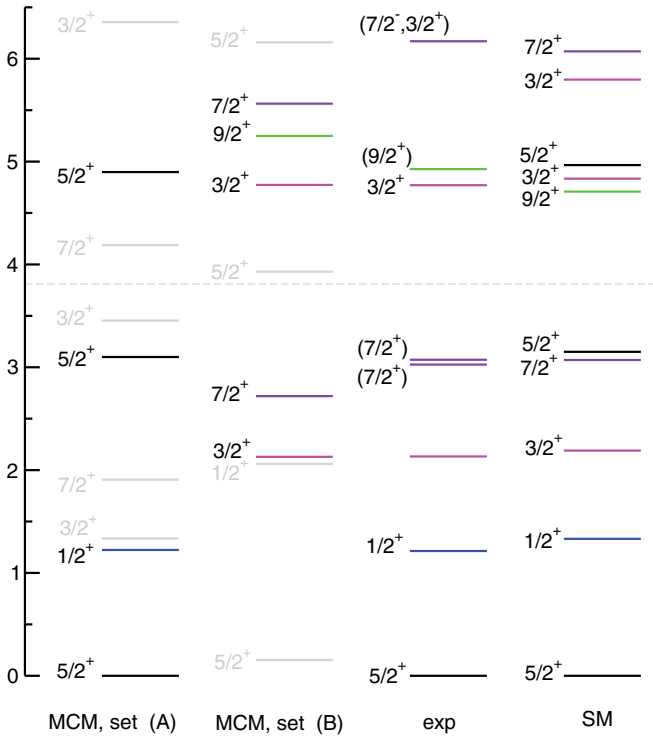

FIG. 3. (Color online) Experimental spectrum of ^{21}O in comparison with the one calculated within the WBP shell model and within the MCM with two different sets of Majorana exchange and the spin-orbit force parameters.

situation with the $1/2^+_1$ is slightly different. Its energy changes only by ∼300 keV when the multichannel MCM is replaced by the single-channel version. This means that the Thomas-Ehrman shift is somehow suppressed by core excitations in the multichannel MCM whereas it is strongly pronounced in the single-channel case. The latter predicts that the excitation energy of the s-wave state $1/2^+_1$ undergoes almost a 1-MeV change in the mirror pair ^{21}O-^{21}Al. This is more than the largest known shift, 725 keV, observed in the ^{19}O$(1/2^+_1)$-^{19}Na$(1/2^+_1)$ mirror pair [15]. No such effect is suggested by multichannel MCM.

To understand if large reduction of the ^{21}Al(g.s.) energy due to core excitations may occur in reality, we have explored two other mirror pairs, ^{21}Ne-^{21}Na and ^{19}O-^{19}Na. We have found out that if experimental neutron separation energies in ^{19}O and ^{21}Ne are reproduced, the mirror proton energies obtained in single-channel MCM are always close to the experimental ones while those obtained in the multichannel MCM are always smaller. The extent of this reduction strongly correlates with the strength of the core excited components. The core excitations in ^{21}Ne-^{21}Na are found to be less important than in ^{19}O-^{19}Na and the deviation of the multichannel MCM proton separation energies from the experimental ones is smaller. The calculated proton resonance energies in ^{19}Na favor the single-channel model for the Coulomb energy difference, whereas the spectra of ^{19,21}O in contrast present a strong evidence for the core polarization. This indicates that the Coulomb shift between mirror states has a complicated nature. Effects that are absent in the current version of the MCM, for example, particle-hole excitations and/or correct asymptotics in the core wave functions, can play an important role in the shift.

The core excitations dominate in the $3/2^+_1$, $5/2^+_2$, and $7/2^+_1$ states of ^{21}O. Their mirrors, in any version of the MCM, lie above the ^{20}Mg(2^+)+p threshold and thus should decay into the ^{20}Mg(2^+) state at 1.598 MeV observed in [16]. For these states, we do not report results from multichannel MCM as it underestimates the 2^+_1 excitation energy in ^{20}O-^{20}Mg by 140–230 keV, however, we perform the single-channel MCM calculations including only the ^{20}O(2^+) + n (^{20}Mg(2^+) + p) channel with all sets of quantum numbers $\{lI_C\}$. In the single-channel MCM, the $3/2^+_1$ and $5/2^+_2$ states are dominated by the s-wave motion around the 2^+ excited core (and thus show noticeable Thomas-Ehrman shift) while $7/2^+_1$ is dominated by d-wave motion. In these calculations the neutron energies with respect to ^{20}O(2^+) were fitted and the resonance energies with respect to the ^{20}Mg(2^+) core were computed. Then the experimental excitation energy of ^{20}Mg(2^+) was

TABLE III. The energies ϵ_p of the resonance states in ^{21}Al calculated in the multichannel and single-channel MCM as well as in two versions of the potential model. The energies (in MeV) are shown with respect to the ^{20}Mg$(0^+_1)+p$ channel. The proton widths $\Gamma^{(dp)}_{0^+}$ and $\Gamma^{(dp)}_{2^+}$ with respect to ^{20}Mg$(0^+_1)+p$ and ^{20}Mg$(2^+_1)+p$ channels, respectively, have been calculated for different values of ϵ_p using Eqs. (1) and (5) and experimental ANC values of the mirror ^{21}O states from Table I. All widths are in keV. Estimated uncertainties of $\Gamma^{(dp)}_{0^+}$ and $\Gamma^{(dp)}_{2^+}$ for ^{21}Al$(5/2^+_1)$,^{21}Al$(1/2^+_1)$, ^{21}Al$(3/2^+_2)$, and ^{21}Al$(7/2^-_2)$ are 15%. The widths Γ_{0^+} calculated in the MCM are also shown.

							Potential model					
	Multichannel MCM			Single-channel MCM			$r_0 = 1.25$ fm, $a = 0.65$ fm			$r_0 = 1.35$ fm, $a = 0.75$ fm		
J_i	ϵ_p	Γ_{0^+}	$\Gamma^{(dp)}_{0^+}$	ϵ_p	$\Gamma^{(dp)}_{0^+}$	$\Gamma^{(dp)}_{2^+}$	ϵ_p	$\Gamma^{(dp)}_{0^+}$	$\Gamma^{(dp)}_{2^+}$	ϵ_p	$\Gamma^{(dp)}_{0^+}$	$\Gamma^{(dp)}_{2^+}$
$5/2^+_1$	0.08	2.1×10^{-14}	1.7×10^{-14}	1.13	0.6		1.21	0.7		0.84	0.06	
$1/2^+_1$	1.09	67	47	1.36	190		1.55	248		1.29	105	
$3/2^+_1$	1.90	0.09	⩽0.016	2.47	⩽0.058	⩽6.7	2.63	⩽0.077	⩽18	2.38	⩽0.048	⩽3.4
$5/2^+_2$	2.79	0.19	⩽3.0	3.29	⩽6.2	⩽7700	3.25	⩽5.9	⩽7000	2.98	⩽4.0	⩽3100
$7/2^+_1$	2.70	9×10^{-6}	⩽0.0004	3.74	⩽0.003	⩽38	3.78	⩽0.003	⩽42	3.39	⩽0.002	⩽15
$3/2^+_2$	4.68	783	412	5.18	570		5.60	743		5.31	636	
$(7/2^-_2)$							6.95	273	167	6.59	193	138

added to get the energy ϵ_p with respect to the $^{20}\mathrm{Mg}(0^+) + p$ threshold shown in Table III.

V. CALCULATIONS OF ^{21}Al RESONANCE ENERGIES IN POTENTIAL MODEL

It is worth mentioning that ϵ_p from the single-channel MCM are very close to the predictions of traditional potential two-body models with the same nuclear potential well in mirror states. Using the standard radius $r_0 = 1.25$ fm and diffuseness $a = 0.65$ fm of the Woods-Saxon potential well, with the depth fitted to reproduce the neutron separation energies in ^{21}O and adding a Coulomb potential of uniformly charged sphere we get the proton resonance energies ϵ_p in ^{21}Al shown in Table III. They are sensitive, however, to the shape of the potential well. Experimentally, enhanced ^{20}Mg interaction cross section was measured [17] suggesting a larger r.m.s. radius for ^{20}Mg. To show what effect a wider potential well can produce on ϵ_p we present a second calculation in Table III with $r_0 = 1.32$ fm and $a = 0.75$ fm. The wider potential well leads to smaller ϵ_p.

Using ϵ_p from Table III and C_n^2 from Table I in Eq. (1) we get the proton widths $\Gamma_{0^+}^{(dp)}$ and $\Gamma_{2^+}^{(dp)}$ for the $^{21}\mathrm{Al} \to {}^{20}\mathrm{Mg}(0^+) + p$ and $^{21}\mathrm{Al} \to {}^{20}\mathrm{Mg}(2^+) + p$ decays shown in Table III. One can see that $\Gamma_{0^+}^{(dp)} \ll \epsilon_p$ for all five analogs of ^{21}O bound states in any version of theory used to calculate ϵ_p. For $3/2_1^+$ and $7/2_1^+$ states, the proton widths $\Gamma_{2^+}^{(dp)}$ are also much smaller than the proton energies with respect to the $^{20}\mathrm{Mg}(2^+) + p$ decay. For $5/2_2^+$ the upper limit for $\Gamma_{2^+}^{(dp)}$ is not meaningful because it is derived from a ratio to the very small predicted cross section for sequential transfer, which is unreliable. There is in fact good reason to suppose that the $5/2_2^+$ resonance should also be very narrow because its single-particle width in the $^{20}\mathrm{Mg}(2^+) + p$ channel is about 40 keV and the corresponding spectroscopic factor is less than one.

VI. WIDTHS OF ^{21}Al STATES

We have estimated energies and widths for mirror analogs of two unbound states seen in the $^{20}\mathrm{O}(d,p)^{21}\mathrm{O}$ reaction at 4.17 and 6.17 MeV. The first unbound state has spin parity $3/2_2^+$, while the spin parity of the second state is not completely clarified. Our previous work suggested that it could be either $3/2^+$ or $7/2^-$ [11]. However, recent analysis in Ref. [18] prefers $7/2^-$. Therefore, in this paper we adopt the $7/2^-$ assignment to make prediction for the mirror analog of the second unbound state. The neutron widths Γ_n of these states have been calculated from spectroscopic factors S, determined as ratios of experimental to theoretical cross sections, and the single-particle neutron width $\Gamma_n^{s.p.}$, $\Gamma_n = S\Gamma_n^{s.p.}$. Γ_n is related to the ANC of the unbound state [19] and for peripheral reactions is independent of the radius r_0 of the neutron potential well, which occurs in our case (see Fig. 1). The total neutron width of $^{21}\mathrm{O}(3/2_2^+)$ extracted from the (d,p) reaction is 80 ± 12 keV while the width for the $^{21}\mathrm{O}(7/2_1^-)$ decay into $^{20}\mathrm{O}(0^+) + n$ and $^{20}\mathrm{O}(2^+) + n$ is 21.0 ± 3.2 keV and 51.0 ± 7.6 keV respectively. The ratio of widths Γ_p and Γ_n for mirror proton and neutron states can be approximated by the ratio of barrier penetration factors $P_l(\epsilon, R_N) = \kappa R_N/(F_l^2(\kappa R_N) + G_l^2(\kappa R_N))$:

$$\Gamma_p/\Gamma_n \approx P_l(\epsilon_p, R_N)/P_l(\epsilon_n, R_N). \quad (5)$$

The energy ϵ_p of $^{21}\mathrm{Al}(3/2_2^+)$ has also been estimated in the multichannel, single-channel MCM and potential models, as for the bound states. As the negative parity states are not well described in the MCM, we apply only the potentials model for the $7/2^-$ state. The predicted spectrum of ^{21}Al is shown in Fig. 4. The energies ϵ_p and corresponding proton widths $\Gamma^{(dp)}$ obtained from Eq. (5) with these energies are presented in Table III. This table again shows that $\Gamma \ll \epsilon_p$ in all predictions.

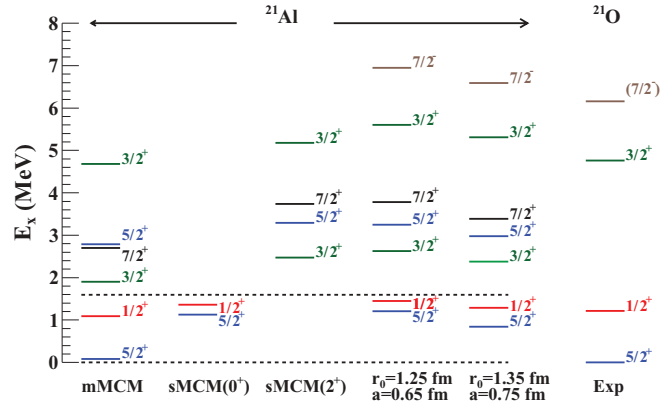

FIG. 4. (Color online) The ^{21}Al spectrum predicted in multi- and single-channel MCM, and in two versions of the potential model in comparison with the mirror spectrum of ^{21}O. Dashed lines denote the $^{20}\mathrm{Mg}(0^+) + p$ and $^{20}\mathrm{Mg}(2^+) + p$ thresholds.

VII. SUMMARY

We have found out that the exotic isotope ^{21}Al beyond the proton dripline should have at least five narrow states which are mirror analogs of the five bound ^{21}O states. The first two are narrow because they are well below the Coulomb barrier but the next three states are narrow because they are built on the first excited state of ^{20}Mg. Two other states around 6 MeV are expected to exist with widths in the range between 100 and 800 keV. These states could be observed via resonance scattering $^{20}\mathrm{Mg} + p$ and three proton transfer reaction $^{18}\mathrm{Ne}(^{12}\mathrm{C},^{9}\mathrm{Li})^{21}\mathrm{Al}$ similar to the $^{18}\mathrm{O}(^{18}\mathrm{O},^{15}\mathrm{O})^{21}\mathrm{O}$ reaction used to study the ^{21}O spectrum in Ref. [20].

ACKNOWLEDGMENTS

N.K.T. and W.N.C. acknowledge the United Kingdom Science and Technology Facilities Council (Grant No. ST/J000051/1). B.F.D. acknowledges financial support from the Ramón y Cajal programme of the Spanish Ministry of Science and Technology.

[1] L. Canton, G. Pisent, J. P. Svenne, K. Amos, and S. Karataglidis, Phys. Rev. Lett. **96**, 072502 (2006).
[2] I. Mukha *et al.*, Phys. Rev. C **79**, 061301(R) (2009); **82**, 054315 (2010).
[3] M. G. Pellegriti *et al.*, Phys. Lett. B **659**, 864 (2008).
[4] N. K. Timofeyuk and P. Descouvemont, Phys. Rev. C **81**, 051301(R) (2010).
[5] R. B. Firestone, Nucl. Data Sheets **103**, 269 (2004).
[6] G. Audi, A. H. Wapstra, and C. Thibault, Nucl. Phys. A **729**, 337 (2003).
[7] B. J. Cole, Phys. Rev. C **58**, 2831 (1998).
[8] L. Prochniak, S. Szpikowski, and W. Berej, J. Phys. G **23**, 705 (1997).
[9] N. K. Timofeyuk, R. C. Johnson, and A. M. Mukhamedzhanov, Phys. Rev. Lett. **91**, 232501 (2003).
[10] N. K. Timofeyuk, P. Descouvemont, and R. C. Johnson, Phys. Rev. C **75**, 034302 (2007).
[11] B. Fernandez-Dominguez *et al.*, Phys. Rev. C **84**, 029902(R) (2011); **84**, 029902(E) (2011).
[12] B. A. Brown, Prog. Part. Nucl. Phys. **47**, 517 (2001); B. A. Brown and W. D. M. Rae, NUSHELL@MSU, MSU-NSCL Report, 2007 (unpublished).
[13] A. B. Volkov, Nucl. Phys. **74**, 33 (1965).
[14] D. Baye and N. Pecher, Bull. Cl. Sc. Acad. Roy. Belg. **67**, 835 (1981).
[15] F. de Oliveira Santos *et al.*, Eur. Phys. J. A **24**, 237 (2005).
[16] A. Gade *et al.*, Phys. Rev. C **76**, 024317 (2007).
[17] L. Chulkov *et al.*, Nucl. Phys. A **603**, 219 (1996).
[18] H. T. Fortune and R. Sherr, Phys. Rev. C **85**, 027305 (2012).
[19] A. M. Mukhamedzhanov and R. E. Tribble, Phys. Rev. C **59**, 3418 (1999).
[20] W. N. Catford *et al.*, Nucl. Phys. A **503**, 263 (1989).